The Surrogate Nuclear Reaction Method: Concept, recent advances, and new opportunities

Jutta E. Escher[1,*]

[1]Nuclear and Chemical Sciences Division, Lawrence Livermore National Laboratory, Livermore, California 94551, USA

Abstract. Cross sections for compound-nuclear (CN) reactions are important for nuclear astrophysics and other applications. Direct measurements are not always possible for the reactions of interest and calculations without experimental constraints can be quite uncertain. Thus indirect approaches, such as the surrogate reaction method (SRM), are being developed to fill the gaps. The SRM, which uses a (direct) inelastic scattering or transfer reaction to obtain information on the decay of a specific compound nucleus, has a long history of providing probabilities for fission, γ, and particle emission. While earlier implementations of the method used minimal theory to provide approximate cross sections for (n,f) reactions, better theoretical descriptions of the underlying reaction mechanisms have made it possible to also obtain (n,γ), (n,n'), and (n,2n) cross sections that agree well with benchmarks. I discuss multiple applications of the modern implementation of the SRM, highlight theory advances that enable them, and comment on opportunities offered at new experimental facilities.

1 Introduction

Many applications in the areas of nuclear astrophysics, nuclear energy, and national security require cross sections for compound-nuclear reactions [1–3]. When reaction data is available, nuclear data evaluators perform calculations to complement the measurements by providing interpolations (mostly in energy), some extrapolations (typically to neighboring isotopes), and estimated uncertainties. Evaluations use a combination of R-matrix and Hauser-Feshbach (HF) reaction theory to describe compound-nuclear (CN) reactions; direct-reaction theory is used to provide transmission coefficients for HF calculations and additional contributions that are not included in the HF description. The discussion in this paper is focused on constraining cross sections for reactions that can be described in the HF formalism. These are reactions that involve statistical averages over strongly overlapping CN resonances [4].

The HF formalism expresses the reaction cross section as a product of the formation cross section and the decay probability:

$$\sigma_{a\chi}(E_a) = \sum_{J,\pi} \sigma_\alpha^{CN}(E_{ex}, J, \pi)\, G_\chi^{CN}(E_{ex}, J, \pi)\, W_{a\chi}(J)\ . \quad (1)$$

Here $\sigma_\alpha^{CN}(E_{ex}, J, \pi)$ describes the formation of the CN at excitation energy E_{ex}, spin J, and parity π, by fusing a projectile a with a target nucleus A and $G_\chi^{CN}(E_{ex}, J, \pi)$ describes the decay of the CN into the channel of interest, χ. The product reflects the fact that the reaction proceeds in two stages – formation and decay of the intermediate CN. The sum runs over all spins and parities (J, π) of the CN. For a neutron capture reaction, $A(n,\gamma)B$, we have $\alpha = n+A$ and $\chi = \gamma$. Corrections to the factorization are encoded in the width fluctuation correction factor, $W_{a\chi}(J)$ [5].

Multiple models are needed to calculate the components in the HF formula: Optical models enable us to calculate the transmission coefficients (TCs) which quantify the fusion of neutrons or charged particles with the target to form the CN, and for the evaporation of these particles from the CN. The probability for the decay into a specific decay channel requires similar TCs for additional particles (e.g. deuterons, α particles, etc.), as well as γ strength functions (γSFs) for the emission of photons, and information on fission barriers for decay by fission. Also needed are level densities in the intermediate and residual nuclei involved in the reaction.

Many models have been developed for use in HF calculations [6]. Most are based on phenomenological descriptions of the underlying nuclear properties and involve adjustable parameters. The multitude of choices that are available can make the calculations quite uncertain, in particular when multiple decay channels compete. Nuclear data evaluators use their subject-matter expertise to select the most appropriate models and rely on experimental data to constrain the model parameters. This becomes a challenge when no data exists, as is typically the case for unstable isotopes, both near and – especially – far away from the valley of stability.

To address this challenge, a multi-pronged approach is needed: 1) We need to develop microscopic theories that are able to predict the structure and reaction ingredients. Such theories use protons, neutrons, nuclear forces, and a quantum-mechanical many-body framework as building blocks. 2) We need to perform direct measurements of

*e-mail: escher1@llnl.gov

the desired reaction cross sections, where possible. 3) We need to obtain constraints from indirect measurements. All three of these components are required: Predictive theory is needed, as it is not feasible (or desirable) to measure every single reaction cross section used in applications. Direct measurement provide stringent tests of theoretical predictions, and indirect measurements are indispensable when direct measurements cannot be carried out.

The surrogate reaction method (SRM) is an approach that combines theory and experiment to provide such indirect constraints for CN reactions. The approach has been used in various forms since the 1970s, when it was introduced to obtain cross sections for neutron-induced fission (see Ref. [7] for a review). Over the past decade, the method has seen much new development, in both experiment and in theory. The focus has shifted from (n,f) reactions to neutron capture, for which there is strong interest, in particular in the nuclear astrophysics community. The approach can also be used for other neutron-induced reactions, e.g. (n,n′), (n,2n), (n,p), (n,α), and for reactions with other incident particles, such as protons or alpha particles. This paper describes the surrogate concept, highlights recent developments, and points out new opportunities.

The SRM formalism and illustrative applications are described in the next section. A central tenet of the modern implementation of the method is the integration of reaction theory, which makes it possible to account for the "spin-parity mismatch" - the difference in the way the intermediate, compound nucleus is populated in the surrogate reaction relative to the population occurring in the desired reaction. This issue is treated in Sect. 3. Opportunities for using the SRM at radioactive beam facilities and for new fission studies are considered in Sects. 4 and 5, respectively. Present limitations of the approach are mentioned in Sect. 6 and concluding remarks are given in Sect. 7.

2 Surrogate reactions method

This section introduces the modern surrogate reactions approach and illustrates the method with examples that employ different surrogate mechanisms, including transfer reactions and inelastic scattering, to obtain cross sections for neutron-induced reactions.

2.1 Concept

The method makes use of the fact that the reaction of interest, $a + A \rightarrow B^* \rightarrow c + C$, proceeds in two stages, with the cross section uncertainties arising primarily from a lack of information on the competing decay channels. To obtain data that constrain the decay models, one performs an alternative 'surrogate' reaction – inelastic scattering or a transfer reaction - that uses a more accessible projectile-target combination to produce the CN B^*: $d + D \rightarrow B^* + b$. More precisely, the reaction initially produces a doorway state (B^d). If the doorway state evolves to the CN ($B^d \rightarrow B^*$), one can measure an observable for the decay channel $B^* \rightarrow c + C$ of interest, in coincidence with the outgoing particle b from the surrogate reaction. Observables used to identify the decay channel may include fission fragments, recoiling reaction remnants, or characteristic γ transitions in the remnant nuclei. The concept is illustrated in Fig. 1 (top) for the ^{92}Zr(p,d) case, which was used to determine the ^{90}Zr(n,γ) cross section [8]. In that case, γ transitions in ^{91}Zr were measured in coincidence with the outgoing deuteron from the (p,d) reaction.

Formally, we express the probability for observing the characteristic decay observable as

$$P_{\delta\chi}(E_{ex}) = \sum_{J,\pi} F_{\delta}^{CN}(E_{ex}, J, \pi)\ G_{\chi}^{CN}(E_{ex}, J, \pi)\ , \quad (2)$$

where $F_{\delta}^{CN}(E_{ex}, J, \pi)$ is the spin-parity population of the CN and δ refers to the formation of the CN in the surrogate reaction. The spins and parities of the CN are those of the doorway state; they depend on the surrogate reaction. Calculations of $F_{\delta}^{CN}(E_{ex}, J, \pi)$ are discussed in Sect. 3.2. As in Eq. (1), $G_{\chi}^{CN}(E_{ex}, J, \pi)$ describes the decay of the CN and contains models with uncertain parameters, such as level densities (LDs) and γ-ray strengths functions (γSFs). By adjusting decay models and parameters to reproduce measured coincidence probabilities, $P_{\delta\chi}(E_{ex})$, one obtains the constraints needed to calculate the desired cross section.

2.2 Direct (p,d) as a surrogate reaction mechanism

The first SRM application that accounted for the spin-parity population of the CN as described above utilized a (p,d) reaction to obtain neutron capture cross sections. The ^{90}Zr(n,γ) and ^{87}Y(n,γ) cross sections were determined using surrogate ^{92}Zr(p,d)^{91}Zr* and ^{89}Y(p,d)^{88}Y* reactions, respectively [8]. The ^{90}Zr capture cross section is known and served as a benchmark for the method. A 28.5 MeV proton beam was impinged on a ^{92}Zr target which produced the ^{91}Zr* CN (see Fig. 1, top). The angle and energy of the outgoing deuteron were used to reconstruct the energy of the CN. The setup made it possible to scan through energies in ^{91}Zr from the ground state to $E_{ex} \approx$14 MeV. In coincidence with the deuteron, characteristic γ-rays, corresponding to transitions between low-lying states in ^{91}Zr were used to identify the decay channel.

Each γ transition yields probability data of the type shown in the bottom panel of Fig. 1. The probability of observing the 1882 keV γ-transition falls off above S_n, since neutron emission becomes competitive. This fall-off provides constraints for the models used in statistical decay calculations for the CN ^{91}Zr, in particular for LDs and γSFs.

To determine the constraints, appropriate spin-parity populations $F_{\delta}^{CN}(E_{ex}, J, \pi)$ are used in Eq. 2 and the parameters in $G_{\chi}^{CN}(E_{ex}, J, \pi)$ are fitted to reproduce the measured coincidence probabilities, $P_{\delta\chi}(E_{ex})$. This was done using Monte-Carlo sampling of a prior distribution for five LD and nine γSF parameters, and applying a Bayesian approach. Subsequently, the desired ^{90}Zr(n,γ) cross section was calculated using parameters sampled from the posterior distribution [8]. The CN formation cross sections $\sigma_{\alpha}^{CN}(E_{ex}, J, \pi)$ were calculated with the Koning-Delaroche optical-model potential [10]. The capture cross section was found to be in good agreement with direct measurements and evaluations [8].

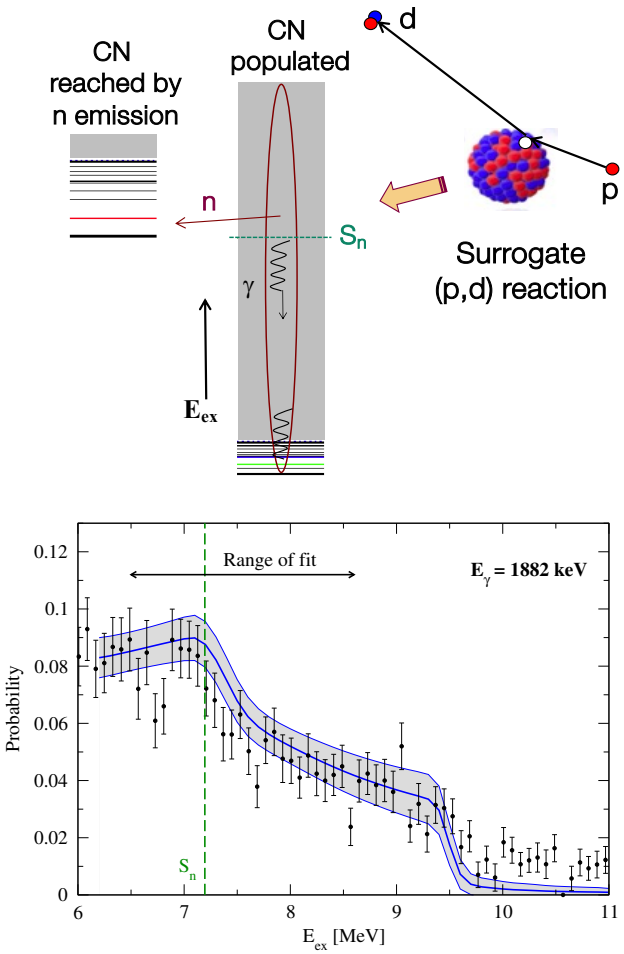

Figure 1. Top panel: The surrogate ^{92}Zr(p,d) reaction was used to produce the CN ^{91}Zr*, which subsequently decayed by neutron evaporation and γ emission. The experiment measured the probability of observing γ transitions between low-lying states in ^{91}Zr in coincidence with the deuteron from the surrogate reaction (Reproduced from Ref. [9].). Bottom panel: Measured coincidence probability for the 1882 keV transition, as function of the ^{91}Zr excitation energy, and fit (grey band) achieved by adjusting parameters in the CN decay models. The resulting parameters were used to extract the ^{90}Zr(n,γ) cross section, see Ref. [8] (©American Physical Society, 2018, reproduced with permission).

The SRM relies only on the surrogate reaction data. In the application discussed, no use was made of auxiliary quantities, such as the average s-wave resonance spacing (D_0) or average radiative width ($\langle\Gamma_\gamma\rangle$) which, if available, provide stringent constraints on the LDs and γSFs, and thus on the (n,γ) cross section. This is important, since - unlike in this benchmark case - D_0 and $\langle\Gamma_\gamma\rangle$ are not available for capture reactions on unstable nuclei. In fact, since the SRM provides constraints for parameters of the LD and γSF models, one can *calculate* D_0 and $\langle\Gamma_\gamma\rangle$. The results are shown in the first line of Table 1. Results from other work, all of which rely on direct measurements of D_0 and $\langle\Gamma_\gamma\rangle$, are shown for comparison. Overall, reasonable agreement is found with the available data.

Table 1. Average s-wave resonance spacing (D_0) and gamma decay width ($\langle\Gamma_\gamma\rangle$), extracted from the analysis of surrogate ^{92}Zr(d,p) data, compared to values from direct measurements.

D_0 [keV]	$\langle\Gamma_\gamma\rangle$ [meV]	Reference
10	185	Surrogate (p,d), Ref. [8]
6.89 (0.53)	170 (20)	Mughabghab, Ref. [15]
6.00 (1.40)	130 (40)	RIPL-3, Ref. [6]
7.18 (23)	180 (137)	Guttormsen, Ref. [14]
7.18 (23)	130 (40)	Guttormsen, Ref. [14]

The parameter constraints determined from the fit to the surrogate (p,d) data also allow for the calculation of the γ-ray strength function. The E1 and M1 γSFs are shown in Fig. 2. The thick curves are the average values, and the grey and orange bands give the uncertainties; the dashed black curve is the total. Results from other measurements are shown for comparison.

Both the capture cross section [8] and the decay models (Fig. 2) compare favorably with other measurements for this n+^{90}Zr benchmark case. This provides confidence for using the method to determine cross sections for reactions on unstable nuclei, such as neutron capture on the short-lived ^{87}Y isotope. Using the same experimental setup as employed for the Zr case, a surrogate ^{89}Y(p,d) experiment was performed. Cross sections were obtained for neutron reactions involving both ground and isomeric states states in ^{87}Y and ^{88}Y [8, 11].

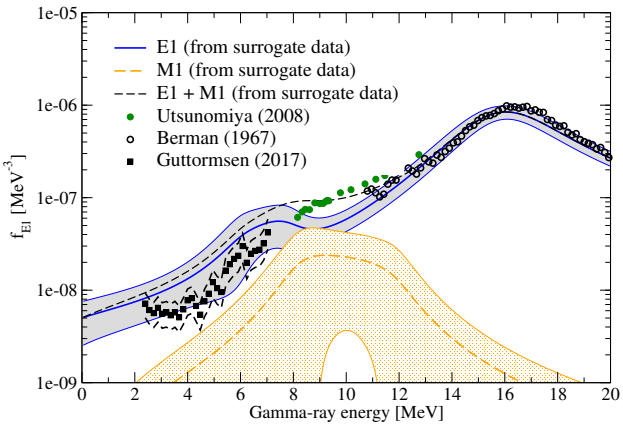

Figure 2. E1 (blue curve, grey band) and M1 (orange band) γ-ray strength functions obtained from surrogate ^{92}Zr(p,d) data, with uncertainties. The sum (dashed black curve) are compared to data by Berman *et al.* [12], Utsonomiya *et al.* [13], and the indirect measurement by Guttormsen *et al.* [14].

2.3 Direct (d,p) as a surrogate reaction mechanism

The second SRM application that accounted for the spin-parity population of the CN in the manner described above employed a (d,p) reaction: A ^{95}Mo(d,p) experiment was performed to obtain the ^{95}Mo(n,γ) cross sections [16].

In regular-kinematics, a (d,p) surrogate reaction has limited use for inferring the cross section of a neutron-induced reaction, since it requires the same target that a

direct measurement of the desired reaction would use. For inverse-kinematics experiments with radioactive beams, however, (d,p) has some attractive attributes: When impinging a heavy unstable beam on a deuterated target, the outgoing protons can be conveniently detected at back angles. In addition, since (d,p) measurements are expected to be used for probing single-particle structure of exotic isotopes, nuclear structure investigations and surrogate measurements can be performed in the same experiment.

The ^{95}Mo(d,p) case was carefully selected to provide a meaningful benchmark: The CN nucleus produced in the surrogate reaction, ^{96}Mo*, is even-even, with a γ-decay pattern that is relatively simple to model in HF decay calculations. Several known γ transitions were observed, including a $2^+ \rightarrow 0^+$ collector transition. The desired ^{95}Mo(n,γ) cross sections has been measured directly over a broad energy range. The cross section extracted from the surrogate experiment was found to be in excellent agreement with the directly-measured result and nuclear data evaluations [16].

2.4 Inelastic scattering as a surrogate reaction mechanism

A third application of the SRM with consideration of the spin-parity population of the CN used inelastic scattering for an actinide nucleus. Perez Sanchez *et al.* [17] performed an inelastic alpha scattering experiment with a ^{240}Pu target and observed the decay of the CN ^{240}Pu*. They measured the probabilities for observing the outgoing α with a) the γ channel and b) the fission channel. Using calculated spin-parity populations, they modeled the CN decay and adjusted parameters in the HF calculation to reproduce the observed γ and fission coincidence probabilities. The extracted fission and capture cross sections were found to be in reasonable agreement with direct measurements. They also demonstrated that not taking into account the differences in the spin-parity populations of the desired and surrogate reactions gives results that deviate significantly from the correct cross section.

Inelastic scattering is known to produce compound nuclei at very high excitation energies, making it an ideal surrogate reaction mechanism for determining (n,n$'$) and (n,2n) cross sections. An experiment for that purpose was performed at LBNL [18]. A 50-MeV ^{3}He beam was used to produce ^{91}Zr* at excitation energies up to $E_{ex} \approx 34$ MeV. At low energies, the ^{91}Zr* nucleus was seen to decay solely by γ emission. Above S_n, neutron emission (followed by γ transitions in ^{90}Zr) started to compete. At even higher energies, two neutrons were emitted and γ transitions in ^{89}Zr were observed. Thus, one surrogate experiment provided information on three exit channels, as identified by γ-transitions in ^{91}Zr, ^{90}Zr, and ^{89}Zr. Utilizing calculated spin-parity populations for the full energy range, LD and γSF parameters were fitted to reproduce the measured surrogate coincidence probabilities. Subsequent sampling of the fitted parameters made it possible to determine the ^{90}Zr(n,γ), ^{90}Zr(n,n$'$), and Zr(n,2n) cross sections from *one* experiment.

For the ^{90}Zr(n,n$'$) and ^{90}Zr(n,2n) reactions, both the total cross section and partial cross sections for populating isomeric final states were obtained. The preliminary results were found to be in good agreement with the directly measured data and available nuclear data evaluations.

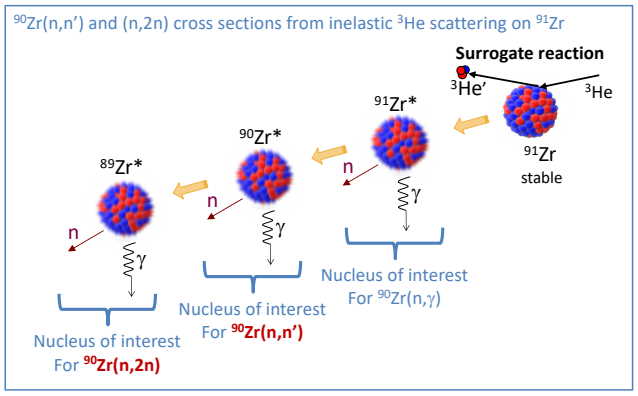

Figure 3. Inelastic ^{3}He scattering was used as a surrogate reaction mechanism to populate the CN ^{91}Zr*. The subsequent decay of the compound nucleus into the channels ^{91}Zr + γ, ^{91}Zr + n and ^{91}Zr + $2n$, was measured by identifying characteristic γ transitions in three residual nuclei, ^{91}Zr, ^{90}Zr, and ^{89}Zr, Using theory to calculate the spin-parity population in ^{91}Zr* and fitting the decay models to reproduce the surrogate data made it possible to obtain the ^{90}Zr(n,γ), ^{90}Zr(n,n$'$), and ^{90}Zr(n,2n), (n,γ) cross sections from this experiment.

3 Spin-parity population of the CN

A CN formed by fusion of a neutron with a target has typically a different (J,π) population than when it is formed via a transfer reaction or inelastic scattering. This is referred to as the 'spin-parity mismatch' or '(J,π) mismatch.' The examples discussed above used calculated surrogate (J,π) populations for the decaying CN to determine the uncertain level density and γ-ray strength function parameters. This procedure is necessary, as the spins and parities populated impact how the CN decays.

3.1 Impact of spin-parity populations on CN decay

The question of how the (J,π) population impacts the decay of the CN has been thoroughly studied. Multiple publications have investigated the behavior of the $G_\chi^{CN}(E_{ex},J,\pi)$ values that occur in Eq. 2, for various (J,π) combinations, as a function of excitation energy in CN. The decay calculations were performed for nuclei for which the LD and γSF models are reasonably well known, in several regions of the nuclear chart.

Some of these sensitivity studies also investigated the impact of ignoring the (J,π) mismatch on cross sections obtained from simulated surrogate experiments. They performed a so-called Weisskopf-Ewing (WE) analysis of the simulated data by assuming that the CN decay is independent of (J,π), *i.e.* $G_\chi^{CN}(E_{ex},J,\pi) \approx \mathcal{G}_\chi^{CN}(E_{ex})$.

In this situation $P^{CN}_{\delta,\chi}(E_{ex}) \approx \mathcal{G}^{CN}_{\chi}(E_{ex})$ holds since $\sum_{J,\pi} F^{CN}_{\delta}(E_{ex}, J, \pi) = 1$ for all energies. In the WE limit, the application of the surrogate method becomes very simple, as the cross section of the desired reaction reduces to $\sigma^{WE}_{\alpha\chi}(E_a) = \sigma^{CN}_{\alpha}(E_{ex})\ \mathcal{G}^{CN}_{\chi}(E_{ex})$, where $\sigma^{CN}_{\alpha}(E_{ex}) = \sum_{J,\pi} \sigma^{CN}_{\alpha}(E_{ex}, J, \pi)$ is the CN formation cross section.

In multiple studies, gamma emission was found to be very sensitive to the (J,π) values of the CN, in particular for nuclei with low level densities, e.g. near shell closures [19–22]. When neutron emission is the only competing channel, the decay pattern is seen to be very sensitive to the low-energy behavior of the s- and p-wave neutron transmission coefficients and the properties of the states in the neighboring nucleus that are energetically accessible.

As a consequence of this sensitivity, neutron capture cross sections extracted from surrogate reaction data under the WE assumption can deviate significantly from the actual cross section. This was demonstrated not only in the sensitivity studies [19–21], but also in multiple applications [16, 17, 22–24]. Even for well-deformed nuclei with high level densities, such as the Gd isotopes, the resulting (n,γ) cross sections were seen to be off by factors of 3-10 [22], and the deviations are expected to be worse for nuclei near closed shells, e.g. for ^{90}Zr.

Calculated fission decay probabilities $G^{CN}_{fiss}(E_{ex}, J, \pi)$, on the other hand, were found to be less sensitive to the CN (J,π) values [25]. This is in line with results from early surrogate applications to (n,f) reactions, which used the WE approximation to determine (n,f) cross sections. The WE approximation, as well the "Ratio" variant thereof [26], was used in almost all applications to fission, including some recent applications [27–29]. Notable exceptions include the work by Younes and Britt [30, 31].

While using the WE or Surrogate Ratio approximation to obtain fission cross sections from surrogate reaction data gives results that are generally in reasonable agreement with direct measurements, discrepancies can occur at low energies ($E_n \leq$ 1-2 MeV), and at the onset of first and second-chance fission [25]. It is therefore recommended that one correct for the (J,π) mismatch in fission applications, if possible.

Sensitivity studies have also been performed to assess the effect of (J,π) populations on CN decay by the emission of one neutron, two neutrons, or multiple protons. This is relevant for applications to (n,n') and $(n,2n)$ reactions [32], and (n,xp) reactions [33, 34]. The studies find that these decays are less sensitive to the CN (J,π) values than γ emission cases, but the WE approximation can generally not be justified.

3.2 Calculating spin-parity populations for surrogate reactions

The (J,π) population of the CN formed in a surrogate reaction depends both on the structure of the nucleus *and* on the reaction mechanism used to produce the CN. This means that the (J,π) population cannot simply be taken to be equal to the (expected) intrinsic spin distribution of the nuclear level density. A simple counterexample is provided by inelastic α scattering, which populates preferentially natural-parity states.

Assuming that a particular surrogate reaction produces a (J,π) population similar to that of an n-induced reaction is not justified. Even in a (d,p) surrogate reaction, which deposits a neutron on a target nucleus, there are reaction processes involving the breakup of the deuteron and the emission of the proton that make the formation of the CN different from what occurs in standard neutron absorption.

To calculate the relevant (J,π) population for a given surrogate reaction, it is necessary to go beyond a simple application of available direct-reaction tools. In the cases studied so far, it was necessary to develop descriptions for nuclear structure properties at excitation energies between 5-15 MeV (for neutron capture applications) and higher (up to about 35 MeV for (n,2n) applications). In addition, two-step reactions were found to play a role.

To calculate the (J,π) population, we recall that a surrogate experiment uses a direct reaction, which produces a doorway state B^d that damps into the relevant CN B^*. We only need to calculate the (J,π) population for B^d, since the damping process preserves energy, spin and parity.

In the (p,d) reaction discussed above, deep neutron holes were created to produce excitation energies near the neutron separation energy (7.19 MeV for ^{91}Zr and 9.35 MeV for ^{88}Y). The location and fragmentation of the holes is not well known, but can be calculated by using information contained in dispersive optical-model potentials (DOMPs). Neutron DOMPs give energy-averaged nuclear properties such as single-particle energies and spectral functions, which can be used in calculations of neutron removal. In addition to 1-step neutron removal, it is necessary to calculate contributions from two-step reactions. In the (p,d) application discussed in Ref. [8] two types of two step-reactions were found to contribute: inelastic proton scattering in the entrance channel, followed by neutron removal, (p,p′)(p′,d), and neutron removal followed by inelastic deuteron scattering in the exit channel, (p,d′)(d′,d). Including both 1-step and 2-step contributions is important for reproducing the measured (p,d) 'singles' cross sections, in magnitude and angular distribution, and for obtaining the proper (J,π) population.

The (d,p) reaction appears - at first glance - to be the ideal surrogate for a neutron-induced reaction, as it deposits a neutron on the same target nucleus. However, the proton that is observed in the surrogate experiment can come from various mechanisms, only one of which is relevant to the application. Elastic deuteron breakup, for example, does not produce the CN of interest, so it has to be calculated and corrected for. The process of interest is one in which the deuteron breaks up into a proton and neutron, with the neutron being absorbed while the proton is observed in the detector. Over the past decade, the development of the proper formalism to describe this process has received much attention. The theory has been developed in parallel by several groups [35–37] and the associated codes were found to give consistent results [38].

In the (n,2n) application discussed above, ^{3}He inelastic scattering was used to populate the ^{91}Zr nucleus at various excitation energies, from the low-lying states to about 35

MeV. The structure of all states that could be reached by inelastic scattering were described using the quasi-particle Random-Phase Approximation (QRPA) with a Skyrme interaction [18, 39, 40]. Using a folding model and an effective α-nucleon interaction, coupling potentials were produced that made DWBA calculations possible. In addition to 1-step inelastic scattering, two-step contributions from (^{3}He,d)(d,^{3}He$'$) and (^{3}He,α)(α,^{3}He$'$) were calculated. At energies above $E_{ex} \approx 10$ MeV, all three contributions were needed to reproduce the measured 'singles' cross section and to calculate the (J,π) population of the CN.

The examples discussed here illustrate the significant progress made in understanding and theoretically describing the surrogate reaction mechanisms that are used to indirectly infer unknown cross sections.

4 Surrogate reactions with radioactive beams

Radioactive-beam facilities provide new opportunities to study properties of exotic nuclei. An important area of application is the measurement of properties that allow us to calculate cross sections for unstable isotopes more reliably. This is of particular interest for gaining insights into the processes that are responsible for the synthesis of the heavy elements [1–3]. Multiple surrogate reactions experiments have already been carried out and are being (or have been) used to determine neutron capture cross sections.

4.1 Experiments utilizing discrete γ transitions

Two (d,p) surrogate reaction experiments with Sr beams were conducted at TRIUMF in Vancouver, Canada. In each, a Sr beam was impinged on a CD_2 target. The protons were detected in the segmented Si array SHARC and a set of HPGe clovers was used to detect coincident γ transitions in the CN. The first of these experiments was used in a study of structural properties of ^{96}Sr [41]; an analysis is underway to investigate if the coincident decay probabilities can be used to determine the ^{95}Sr(n,γ) cross section. The second experiment [42] was designed to determine the ^{93}Sr(n,γ) cross section and provide some insights into the decay of the ^{94}Sr nucleus, which was found to emit a surprisingly large number of gammas when produced by β-decay [43]. The analysis for this experiment is underway.

4.2 Experiments detecting recoiling nuclei

While the TRIUMF measurement tagged the channel of interest using γ-rays, an inverse-kinematics ^{84}Se(d,p) experiment conducted at the NSCL detected beam-like recoils in the S800 spectrometer and protons in the ORRUBA barrel array [44] (see Fig. 4). Unreacted beam particles, ^{84}Se, as well as ^{85}Se formed in the (d,p) reaction, and ^{84}Se, resulting from the formation of ^{85}Se with subsequent neutron emission, moved through the spectrometer. A blocker was used to detect only ^{85}Se, the nucleus of interest for the γ channel, in coincidence with protons. The measurement provided the probability for decay into the γ channel, rather than for decay through a specific γ transition in ^{85}Se, but the procedure for determining the ^{84}Se(n,γ) cross section was analogous to that used for the earlier experiments. The preliminary cross section for this unstable isotope was found to be similar to, but lower than the best available calculation, the TENDL23 evaluation, which relies on a combination of microscopic structure predictions and extrapolated regional systematics.

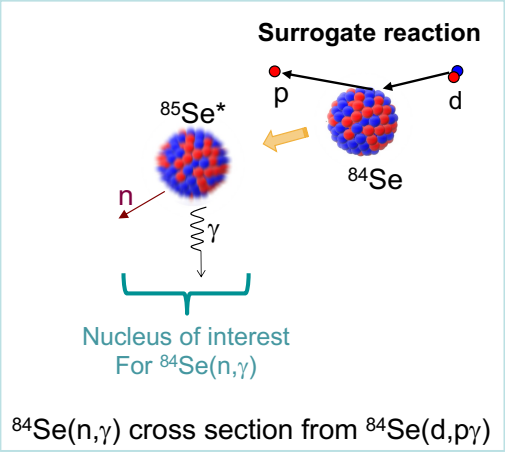

Figure 4. Schematic depiction of an ^{84}Se(d,p) reaction that was carried out in inverse kinematics to obtain the (n,γ) cross section for ^{84}Se, which is two neutrons away from the next stable Se isotope. In the experiment, recoiling beam-like particles (here ^{85}Se) were detected instead of γ transitions in the remnant nucleus.

An inverse-kinematics (d,p) surrogate reaction experiment that similarly focused on detecting recoils was conducted at RIKEN [45]. ^{77,79}Se beams were produced at the BigRIPS separator and impinged on a CD_2 target. Residual Se nuclei were detected in the SHARAQ spectrometer, in coincidence with protons that were identified in a Si strip detector. Estimated (J,π) populations were used in Hauser-Feshbach decay calculations and LD parameters were adjusted to reproduce the surrogate decay probabilities. The parameters constrained in this manner were used to calculate the ^{79}Se(n,γ) cross section. In addition, a variant of the WE approximation, the Surrogate Ratio method, was used to obtain the neutron capture cross section for ^{79}Se relative to that for ^{77}Se.

An inelastic proton scattering experiment was conducted in inverse kinematics at the heavy-ion storage ring at GSI/FAIR [46]. ^{208}Pb ions were accelerated in the ring and intersected with a hydrogen gas target. The inelastically-scattered protons were detected in a Si telescope and beam-like residual recoils were detected in a double-sided strip detector. The probability for observing the neutron channel, which competes with γ decay of ^{208}Pb, was determined as function of the ^{208}Pb excitation energy. Predicted (J,π) populations were combined with HF decay models to calculate the probability of neutron evaporation. Multiple combinations of LDs and γSFs were found to result in good agreement with the measured probabilities. These were also seen to provide cap-

ture cross sections that are in agreement with the evaluated ^{207}Pb(n,γ) cross section.

5 Revisiting fission

Describing the fission process and the various fission observables is a challenge for nuclear theory. Descriptions presently in use range from phenomenological models with adjustable parameters to microscopic static or time-dependent approaches that aim to predict observables. A large amount of data is needed to constrain the parameters and test the theory predictions. In addition, many applications require fission cross sections, fission fragment distributions, and associated observables.

Surrogate reactions can contribute useful information in this context, since various fission properties can be observed in coincidence with the surrogate-reaction ejectile. The approach provides control over the energy of the fissioning nucleus and makes it possible study fission below the neutron threshold. The early surrogate reactions measurements, performed in the 1970s, were focused on obtaining (n,f) cross sections (for a review, see Ref. [7]).

Both the early (n,f) measurements, as well as more recent fission applications [27–29], employed the Weisskopf-Ewing approximation in the analyses of the surrogate data. The recent measurements often used the Surrogate Ratio method, a variant of the WE approximation [26]. The work by Younes and Britt [30, 31] is notable, as it incorporated corrections for the (J, π) mismatch in a re-analysis of older data. More recently, the role of width fluctuations in fission applications has been theoretically investigated [47].

Multiple new opportunities are emerging for studying fission properties with surrogate reactions. At Argonne National Laboratory, the solenoidal spectrometer HELIOS was used in an inverse-kinemematics (d,p) experiment in which a ^{238}U beam impinged on a CD_2 target [48]. The outgoing protons were deflected in the magnetic field and detected upstream in a Si array, while the fission fragments were detected downstream in gas-filled heavy-ion detectors. The resulting coincidence probabilities were used to extract fission barriers for ^{239}U, which in turn were compared to the barriers used in nuclear reaction evaluations. The idea of using a solenoidal spectrometer with a radioactive beam has received a lot of interest. Future measurements are planned with SOLARIS at FRIB and with the ISOLDE Solenoidal Spectrometer at CERN.

6 Present limitiations of the method

The surrogate reaction method is a powerful approach for studying decay properties of compound nuclei. When considering new applications, it is important to keep the present limitations of the method in mind.

Most importantly, the method outlined here can only be used to determine a cross section of a reaction that can be described in Hauser-Feshbach theory, *i.e.* as an average over strongly-overlapping resonances. Compound-nuclear reaction that proceed through the formation of resolved or weakly-overlapping resonances are not expected to be reliably extracted from a surrogate experiment. This applies, for example, to reactions of astrophysical interest that are dominated by individual resonances. The SRM is also not able to provide cross section constraints for direct reactions, such as direct neutron capture.

The surrogate reaction employed has to form a doorway state that damps into the CN of interest. More work is needed to better understand the equilibration process. In addition, practitioners of the method need to critically examine experimental observables for indications of pre-equilibrium decays (which, in some circumstances, can be accounted for).

Finally, the SRM is not a substitute for theoretical approaches that predict reactions. Since it is not possible to measure all reactions of interest, due to the sheer number of them, it is important to develop theoretical predictions for CN reactions. The SRM can then provide targeted cross section results to validate theory and address specific needs.

7 Outlook and conclusions

The surrogate reaction method combines theory and indirect measurements to constrain cross section calculations for compound reactions that cannot be measured directly. The method employs inelastic scattering or transfer reactions in regular or inverse kinematics to form the CN of interest and measures the decay of the CN. The surrogate analysis relies on observables that indicate CN decay into a specific channel of interest to determine parameter constraints needed to calculate the desired cross section. It does not use auxiliary quantities (such as D_0 or $\langle\Gamma_\gamma\rangle$), which are unavailable for unstable isotopes. When Bayesian parameter inference is implemented, it is straightforward to obtain quantified uncertainties and correlations along with the desired cross section.

A critical element for obtaining reliable cross sections is the use of theory to account for the spin-parity mismatch between the surrogate and desired reactions. The last decade has seen significant progress in this area. The development of theoretical descriptions of the surrogate reaction mechanisms has made it possible to extract cross sections for challenging reactions, such as neutron capture, from surrogate data. Additional work is required to efficiently and reliably determine many unknown cross sections of interest. This includes the development of broadly-applicable descriptions of inelastic scattering and transfer reactions, including for deformed nuclei, a better understanding of the equilibration mechanism in nuclei, and the role of width fluctuations in surrogate reactions.

I gratefully acknowledge valuable contributions from my collaborators, theorists F.S. Dietrich, O.C. Gorton, G. Potel, I.J. Thompson, W. Younes, and experimentalists R.J. Casperson, J.A. Cizewski, J.T. Harke, R. Hughes, S. Pain, A. Ratkiewicz, J.J. Ressler, and N.D. Scielzo. This work was performed under the auspices of the U.S. Department of Energy by Lawrence Livermore National Laboratory under Contract DE-AC52-07NA27344, with support from LDRD projects 19-ERD-017, 21-LW-032, 22-LW-029, 23-SI-004, and 24-ERD-023.

References

[1] B.A. Brown, A. Gade, S.R. Stroberg et al., Motivations for Early High-Profile FRIB Experiments (2024). https://arxiv.org/abs/2410.06144

[2] H. Schatz, A.D.B. Reyes, A. Best et al., J. Phys. G: Nucl. Part. Phys. **49**, 110502 (2022). 10.1088/1361-6471/ac8890

[3] A. Arcones et al., Prog. Part. Nucl. Phys. **94**, 1 (2017). 10.1016/j.ppnp.2016.12.003

[4] S. Hilaire, S. Goriely, Towards More Predictive Nuclear Reaction Modelling, in *Compound-Nuclear Reactions*, ed. J. Escher et al. (Springer, 2021), pp. 3–15

[5] S. Hilaire, C. Lagrange, A.J. Koning, Annals of Physics **306**, 209 (2003). DOI: 10.1016/S0003-4916(03)00076-9

[6] R. Capote, et al., Nuclear Data Sheets **110**, 3107 (2009). DOI: 10.1016/j.nds.2009.10.004

[7] J.E. Escher, J.T. Burke, F.S. Dietrich et al., Rev. Mod. Phys. **84**, 353 (2012). 10.1103/RevModPhys.84.353

[8] J.E. Escher et al., Phys. Rev. Lett. **121**, 052501 (2018). 10.1103/PhysRevLett.121.052501

[9] Escher, J. E., Tonchev, A. P., Burke, J. T. et al., EPJ Web of Conferences **122**, 12001 (2016). 10.1051/epjconf/201612212001

[10] A.J. Koning, J.P. Delaroche, Nucl. Phys. **A713**, 231 (2003).

[11] J.E. Escher, Tech. Rep. LLNL-TR-701412, Lawrence Livermore National Laboratory (2016)

[12] B.L. Berman, J.T. Caldwell, R.R. Harvey et al., Phys. Rev. **162**, 1098 (1967). 10.1103/PhysRev.162.1098

[13] H. Utsunomiya et al., Phys. Rev. Lett. **100**, 162502 (2008). 10.1103/PhysRevLett.100.162502

[14] M. Guttormsen et al., Phys. Rev. C **96**, 024313 (2017). 10.1103/PhysRevC.96.024313

[15] S.F. Mughabghab, *Atlas of Neutron Resonances, Resonance Parameters and Thermal Cross Sections Z=1-100*, 5th edn. (Elsevier, Amsterdam, 2006)

[16] A. Ratkiewicz, J.A. Cizewski, J.E. Escher et al., Phys. Rev. Lett. **122**, 052502 (2019). 10.1103/PhysRevLett.122.052502

[17] R. Pérez Sánchez, B. Jurado, V. Méot et al., Phys. Rev. Lett. **125**, 122502 (2020). 10.1103/PhysRevLett.125.122502

[18] J.E. Escher, Tech. Rep. LLNL-TR-839279, Lawrence Livermore National Laboratory (2022)

[19] C. Forssén, F. Dietrich, J. Escher et al., Phys. Rev. C **75**, 055807 (2007) 10.1103/PhysRevC.75.055807

[20] J.E. Escher, F.S. Dietrich, Phys. Rev. C **81**, 024612 (2010). 10.1103/PhysRevC.81.024612

[21] S. Chiba, O. Iwamoto, Phys. Rev. C **81**, 044604 (2010). 10.1103/PhysRevC.81.044604

[22] N.D. Scielzo, J.E. Escher, J.M. Allmond et al., Phys. Rev. C **81**, 034608 (2010). 10.1103/PhysRevC.81.034608

[23] G. Boutoux, B. Jurado, V. Méot et al., Phys. Lett. B **712**, 319 (2012). 10.1016/j.physletb.2012.05.012

[24] Q. Ducasse, B. Jurado, M. Aïche et al., Phys. Rev. C **94**, 024614 (2016). 10.1103/PhysRevC.94.024614

[25] J.E. Escher, F.S. Dietrich, Phys. Rev. C **74**, 054601 (2006). 10.1103/PhysRevC.74.054601

[26] C. Plettner et al., Phys. Rev. C **71**, 051602(R) (2005).

[27] R.O. Hughes, C.W. Beausang, T.J. Ross et al., Phys. Rev. C **85**, 024613 (2012). 10.1103/PhysRevC.85.024613

[28] R.O. Hughes, C.W. Beausang, T.J. Ross et al., Phys. Rev. C **90**, 014304 (2014). 10.1103/PhysRevC.90.014304

[29] R.J. Casperson, J.T. Burke, N.D. Scielzo et al., Phys. Rev. C **90**, 034601 (2014). 10.1103/PhysRevC.90.034601

[30] W. Younes, H.C. Britt, Phys. Rev. C **67**, 024610 (2003). 10.1103/PhysRevC.67.024610

[31] W. Younes, H.C. Britt, Phys. Rev. C **68**, 034610 (2003). 10.1103/PhysRevC.68.034610

[32] O.C. Gorton, J.E. Escher, Phys. Rev. C **107**, 044612 (2023). 10.1103/PhysRevC.107.044612

[33] A. Sharma, A. Gandhi, A. Kumar, Phys. Rev. C **105**, 014624 (2022). 10.1103/PhysRevC.105.014624

[34] A. Sharma et al., Phys. Lett. B **848**, 138381 (2024). 10.1016/j.physletb.2023.138381

[35] G. Potel, F.M. Nunes, I.J. Thompson, Phys. Rev. C **92**, 034611 (2015). 10.1103/PhysRevC.92.034611

[36] J. Lei, A.M. Moro, Phys. Rev. C **92**, 044616 (2015). 10.1103/PhysRevC.92.044616

[37] B.V. Carlson, R. Capote, M. Sin, Few-Body Systems **57**, 307 (2016). 10.1007/s00601-016-1054-8

[38] G. Potel, G. Perdikakis, B.V. Carlson et al., Eur. Phys. J. A **53**, 178 (2017).

[39] G.P.A. Nobre, F.S. Dietrich, J.E. Escher et al., Phys. Rev. Lett. **105**, 202502 (2010). 10.1103/PhysRevLett.105.202502

[40] G.P.A. Nobre, F.S. Dietrich, J.E. Escher et al., Phys. Rev. C **84**, 064609 (2011). 10.1103/PhysRevC.84.064609

[41] S. Cruz, P. Bender, R. Krücken et al., Phys. Lett. B **786**, 94 (2018). 10.1016/j.physletb.2018.09.031

[42] A. Richard et al., Impact of the Experimentally Constrained ^{93}Sr(n,γ)^{94}Sr Reaction for the Astrophysical i-Process, in *APS Meeting Abstracts* (2023)

[43] J.L. Tain, E. Valencia, A. Algora et al., Phys. Rev. Lett. **115**, 062502 (2015). 10.1103/PhysRevLett.115.062502

[44] H. Sims, Ph.D. thesis, Rutgers University (2021)

[45] N. Imai et al., Phys. Lett. B **850**, 138470 (2024). 10.1016/j.physletb.2024.138470

[46] M. Sguazzin, B. Jurado, J. Pibernat et al., First measurement of the neutron-emission probability with a surrogate reaction in inverse kinematics at a heavy-ion storage ring (2024), https://arxiv.org/abs/2312.13742

[47] O. Bouland, P. Marini, Nucl. Data Sheets **193**, 105 (2024). 10.1016/j.nds.2024.01.005

[48] S.A. Bennett et al., Phys. Rev. Lett. **130**, 202501 (2023). 10.1103/PhysRevLett.130.202501